

Antibacterial Activity of Ginger (*Zingiber officinale*) Leaves Essential Oil Nanoemulsion against the Cariogenic *Streptococcus mutans*

Nada M. Mostafa

Department of Pharmacognosy, Faculty of Pharmacy, Ain Shams University, Cairo, Egypt.

ARTICLE INFO

Article history:

Received on: 23/02/2018

Accepted on: 11/07/2018

Available online: 30/09/2018

Key words:

Zingiber officinale, essential oil, GC/MS, *Streptococcus mutans*, molecular docking.

ABSTRACT

Zingiber officinale Roscoe leaves oil was hydrodistilled and analyzed by gas chromatography/mass spectrometry for the first time from the Egyptian chemotype. Ninety compounds (96.63% of total peak area) were identified. Methyl cinnamate (29.21%) represented the most abundant oxygenated compound. Monoterpene hydrocarbons (23.83%) were rich in β -pinene (8.59%) and terpinolene (7.46%). δ -Cadinene (7.05%) represented the majority of sesquiterpene hydrocarbons (20.86%). A nanoemulsion (diameter of 151.4 nm) was formulated by a low-energy method using Tween-80 as a surfactant, with a polydispersity index of 0.27, the zeta potential of -13.75 mV and pH value of 4. Transmission electron microscopy (TEM) confirmed the nanometric-sized particles. The formulation was stable by keeping in the refrigerator for one month. The nanoemulsion antimicrobial activity was tested against *Streptococcus mutans* (compared to clindamycin) with MIC value of $62.5 \mu\text{L/mL}$, confirmed by TEM showing bacterial scattering with impaired biofilm formation, and by in-silico molecular docking of methyl cinnamate to the C-terminal region of *S. mutans* surface protein antigen. To our knowledge, the formulation and its anticariogenic activity validation were carried out for the first time. Thus, ginger leaves oil is rich in valuable phytoconstituents; its nanoemulsion showed efficacy on *S. mutans*, yet further studies are required for testing its applicability as a gargle.

INTRODUCTION

Zingiber officinale Roscoe (family Zingiberaceae) is widely cultivated for its medicinal uses and as a condiment. It is used traditionally to treat the common cold, headache, muscular and rheumatic disorders (Yang *et al.*, 2009). Numerous studies have investigated the phytochemical composition of its rhizomes, revealing zingiberene, gingerol, shogaol and their derivatives as the major components (Sivasoathy *et al.*, 2011). Reported pharmacological activities on ginger include antimicrobial, antioxidant, anti-inflammatory, hepatoprotective and antinociceptive (Abdel Azeem *et al.*, 2013; Jeena *et al.*, 2013; Mostafa and Singab, 2016).

Nanoemulsions are emulsions with sub-micron size that can be produced by either high- or low-energy method. The high energy method involves the application of high-pressure

homogenization or micro-fluidization, while the low energy method involves continuous stirring of a mixture of oil, water, and surfactant, without any drastic condition or expensive equipment (Salama *et al.*, 2016). The choice of the suitable surfactant is important, such as Tween-80, which is a low molecular weight non-ionic surfactant commonly used in food and pharmaceutical products (Salama *et al.*, 2016; Nielsen *et al.*, 2016).

The encapsulation of an essential oil in a nanoemulsion form, protects its thermolabile components, that are also sensitive to the effects of light, moisture, and air and guarantees significant decrease in their volatility, increase of their bioavailability and efficacy as a result of increasing the surface area and stability of the particles (Amaral and Bhargava, 2015; Nantararat *et al.*, 2015).

Dental caries is an oral infection manifested by teeth enamel demineralization and destruction (Hasan *et al.*, 2014). Its main causative agent is *Streptococcus mutans*, which is a colonizing and biofilm-forming bacterium with a high ability to adhere to solid surfaces (Krzyściak *et al.*, 2014). These properties may be attributed to the bacterial ability to survive and tolerate the acids produced as a result of oral carbohydrate metabolism (Hasan

*Corresponding Author

Nada M. Mostafa, Assistant Professor, Department of Pharmacognosy, Faculty of Pharmacy, Ain Shams University, Cairo 11566, Egypt.

E-mail: nadamostafa@pharma.asu.edu.eg

et al., 2015). Dental plaque is the aggregate bacterial accumulation on the surface of teeth, where *Streptococcus mutans* is involved in its development and accumulation (Loesche, 1986).

The aim herein is profiling the volatile components of *Zingiber officinale* leaves, for the first time, from the Egyptian plant; testing the stability, anticariogenic and antiplaque effects of a formulated nanoemulsion of the ginger leaves essential oil against *Streptococcus mutans*, which was carried out for the first time as well. The antimicrobial and antibiofilm-forming activities were supported by transmission electron microscope imaging and an *in-silico* molecular docking study.

MATERIALS AND METHODS

Plant material

Leaves of *Zingiber officinale* Roscoe, family Zingiberaceae were collected from El-Orman Botanical Garden, Cairo, Egypt. Identification of the plant was confirmed by Prof. Dr. Mohamed El Gebaly, Professor of Taxonomy, National Research Centre, Egypt. A voucher specimen was deposited at the Department of Pharmacognosy, Faculty of Pharmacy, Ain Shams University, Abbassia, Cairo, Egypt (PHG-P-ZO-1).

Isolation of volatile component

Fresh plant material (1 Kg) was hydrodistilled in a Clevenger-type apparatus for 4 hours. The resulting yellow oil (0.15% v/w) was then dried over anhydrous sodium sulfate and kept in separately sealed vials at -30°C until analysis.

Essential oil GC-MS analysis

The mass spectrum was recorded by using Shimadzu GC MS-QP2010 (Tokyo, Japan) equipped with Rtx-5MS fused bonded column (30 m \times 0.25 mm i.d. \times 0.25 μm film thickness) (Restek, USA) and a split-splitless injector. The capillary column was directly coupled to a quadrupole mass spectrometer (SSQ 7000; Thermo-Finnigan, Bremen, Germany). The initial column temperature was kept at 45°C for 2 minutes (isothermal), programmed to 300°C at a rate of $5^{\circ}\text{C}/\text{min}$ and kept constant at 300°C for 5 minutes (isothermal). The helium carrier gas flow rate was 1.41 mL/min. The injector temperature was 250°C . The mass spectrum was recorded by applying filament emission current of 60 mA, ionization voltage of 70 eV, and 200°C ion source. A diluted sample (1% v/v) was injected with split mode with a split ratio of 1:15.

Nanoemulsion formulation

The nanoemulsion was prepared by spontaneous emulsification, composed of essential oil (1% v/v); water phase containing Tween-80 (4.5% v/v); then the water was added to complete the volume to 100% v/v. It was kept under moderate magnetic stirring for 5 min at room temperature. The surfactant percentage was determined after several trial and error experiments until reaching a visually homogenous emulsion with no phase separation.

Nanoemulsion characterization

Particle size, PDI, zeta potential and pH determinations

The particle size, polydispersity index (PDI) and charge

of the prepared nanoemulsion were measured (in triplicates) by photon correlation spectroscopy (based on dynamic light scattering), using Zetasizer NanoZS 3600 (Malvern Instruments Ltd., Worcestershire, UK), after adequate aliquot dilution of the samples in distilled water (Manconi *et al.*, 2011). The pH values of the nanoemulsion were determined (in triplicate) directly using a pH meter (Jenway pH meter, Model 3310, UK) at room temperature.

Stability study for the prepared vesicles

The prepared nanoemulsion was stored for one month at a refrigeration temperature of $2-8^{\circ}\text{C}$. During the storage period, the sample was regularly inspected visually for its homogeneity and consistency. The particle size, zeta potential, and polydispersity index (PDI) of the nanoemulsion were also re-measured.

Morphological analysis by transmission electron microscope (TEM)

The nanoemulsion, after appropriate dilution with distilled water, was adsorbed on a carbon-coated copper grid. Then, particles morphology and size were examined and photographed using a JEM 1200 EXII transmission electron microscope, Jeol, Japan, operated at an accelerating voltage of 60-70 KV.

Antimicrobial activity

Microbial strain

The nanoemulsion was tested against *Streptococcus mutans* ATCC 25175.

Agar diffusion method

S. mutans inoculum (density of 0.5% McFarland) was spread on the surface of Brain Heart Infusion agar (Lab M, UK), then tested via the agar diffusion method, according to CLSI methodology (2013). A negative control (containing Tween-80) was prepared as the nanoemulsion but without the essential oil. Ready discs of Clindamycin (2 $\mu\text{g}/\text{disc}$; Bioanalyse, Turkey) were used as positive control. The plates were incubated at 37°C . Each test was performed in triplicate and the results were provided as mean values in mm \pm SD.

Minimum inhibitory concentration (MIC) determination

Broth microdilution method was used for the determination of minimum inhibitory concentration, according to CLSI methodology (2015), by the visual inspection of the microtiter plates (in two-fold dilutions) using a concave mirror for the absence of turbidity.

Morphological analysis by Transmission Electron Microscope (TEM)

The *Streptococcus mutans* suspension was photographed with and without the addition of MIC concentration of the nanoemulsion, on a carbon-coated copper grid using JEM 1200 EXII TEM, Jeol, Japan, operated at an accelerating voltage of 60-70 KV.

Molecular modeling

In-silico molecular modeling was done using Discovery Studio 2.5 software (Accelrys Inc., San Diego, CA, USA) and

applying the C-Docker protocol. The X-ray crystal structure of the C-terminal region of a *Streptococcus mutans* surface protein antigen (PDB ID3QE5) co-crystallized with its ligand has been downloaded from the protein data bank. The program protein preparation protocol and CHARMM force field were applied then the C-Docker binding energy of the selected docking pose was calculated by the program.

Statistical analyses

The results were measured in triplicates and reported as the mean value \pm SD. The statistical analyses were made by unpaired *t*-test using GraphPad InStat 3 Software, Inc. La Jolla, CA, USA. The statistical significance level was set for all analyses at $P < 0.05$.

RESULTS AND DISCUSSION

Essential oil analysis

Ninety compounds constituting 96.63% of the total peak area were identified in the ginger leaves oil by GC/MS analysis, as shown in Table 1, for the first time from the Egyptian chemotype. Methods for compounds identification were their experimental retention indices and mass spectra comparison with the 8th edition of Wiley Registry of Mass Spectral Data, NIST Mass Spectral Library (December 2005), previously published literature (Ayoub *et al.*, 2010; Singab *et al.*, 2014; Mostafa *et al.*, 2015; Mostafa *et al.*, 2018) and/or authentic samples. The major components were oxygenated compounds from different classes (30.38%), of which methyl cinnamate (29.21%) represented the most abundant compound. Monoterpene hydrocarbons (23.83%) represent the second major class of compounds, rich in β -pinene (8.59%) and terpinolene (7.46%). While sesquiterpene hydrocarbons reached 20.86%, of which δ -cadinene (7.05%) was the major component.

A previous study done by Sivasothy *et al.* (2011) on *Z. officinale* var. rubrum Thielade from Malaysia identified forty-six compounds from the leaves oil. They have reported, in common with the present study, the abundance of high percentages of sesquiterpenoids (47.1%), as well as monoterpenoids (42.6%) in the leaves oil. β -caryophyllene represents the major component (31.7%) in their study, while in the present study, β -caryophyllene was detected with only 2.17%. However, our main oil component, methyl cinnamate (29.21%), was not detected at all in their corresponding study. Of the major components identified in the present study; β -pinene, δ -cadinene, and linalool were also identified in their leaves volatiles, but in much lower amounts representing only 2, 0.3 and 1.1%, respectively. Sivasothy *et al.* (2011) didn't detect terpinolene in their leaves oil but they rather identified it in the rhizomes oil. These variations in the leaves oil composition between the two studies may be attributed to the source, method of cultivation, regional variations and the season of plant collection (Sari *et al.*, 2006).

Nanoemulsion characterization

Determination of particle size, distribution, zeta potential and pH

The nanoemulsion particles had a mean diameter of 151.4 nm and a polydispersity index of 0.27, which indicate a homogenous formulation. The particle size distribution is presented in Figure 1. The mean zeta potential value was -13.75

± 3.18 mV, this negative value may be explained by the use of a hydrophilic emulsifier, which is Tween-80 with oxygen atoms in its molecule, that present a negative surface charge density (Flores *et al.*, 2011). The mean pH value of a triplicate measurement of the formulation was 4.

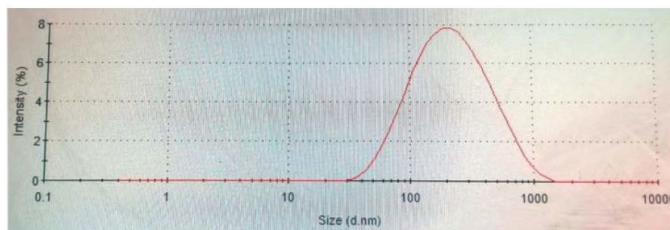


Fig. 1: Nanoemulsion particle size distribution by intensity.

Nanoemulsion stability study

The formulated nanoemulsion was kept in the refrigerator and tested for stability for a period of one month. The stability parameters are presented in Table 2. The nanoemulsion was homogenous and consistent with no apparent phase separation when inspected visually. Non-significant changes in particle size diameter, polydispersity index, and zeta potential were observed after one-month storage ($P < 0.05$).

Morphological analysis using transmission electron microscope (TEM)

TEM examination of the nanoemulsion showed particles of almost spherical shape and confirmed the particles nanometric size, as shown in Figure 2. The particles size observed by TEM was much smaller than that measured by the photon correlation spectroscopy due to the drying process involved in the sample preparation for TEM imaging, thus the dried oil droplets in the core would appear smaller (Ishak *et al.*, 2017; Nantarat *et al.*, 2015).

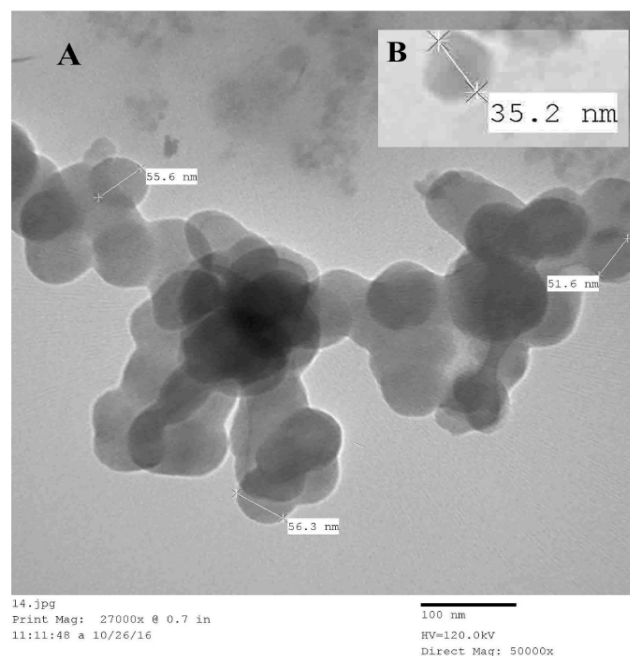


Fig. 2: Transmission electron microscope imaging showing (A) the nanoemulsion (sample magnification was 50000 times); (B) an individual droplet.

Table 1: The chemical composition of ginger (*Zingiber officinale*) leaves volatile oil.

	Compound ^a	RI ^b calculated	RI reported	Composition ^c (%)	Molecular formula	Method of identification
1	α -Pinene	927	929	1.84	C ₁₀ H ₁₆	RI, MS, AU
2	Camphene	943	943	1.46	C ₁₀ H ₁₆	RI, MS
3	Benzaldehyde	958	962	0.01	C ₇ H ₆ O	RI, MS
4	β-Pinene	976	979	8.59	C₁₀H₁₆	RI, MS, AU
5	β -Myrcene	990	992	0.82	C ₁₀ H ₁₆	RI, MS
6	δ -2-Carene	1001	998	0.01	C ₁₀ H ₁₆	RI, MS
7	α -Phellandrene	1004	1007	0.34	C ₁₀ H ₁₆	RI, MS, AU
8	3-Carene	1010	1011	0.33	C ₁₀ H ₁₆	RI, MS
9	α -Terpinene	1017	1017	0.11	C ₁₀ H ₁₆	RI, MS
10	<i>m</i> -Cymene	1023	1022	0.01	C ₁₀ H ₁₄	RI, MS
11	<i>p</i> -Cymene	1025	1025	0.45	C ₁₀ H ₁₄	RI, MS
12	Limonene	1030	1032	2.19	C ₁₀ H ₁₆	RI, MS, AU
13	Eucalyptol	1032	1031	1.58	C ₁₀ H ₁₈ O	RI, MS, AU
14	<i>cis</i> - β -Ocimene	1038	1037	0.01	C ₁₀ H ₁₆	RI, MS
15	<i>trans</i> - β -Ocimene	1049	1050	0.02	C ₁₀ H ₁₆	RI, MS
16	γ -Terpinene	1060	1060	0.15	C ₁₀ H ₁₆	RI, MS
17	Terpinolene	1092	1089	7.46	C₁₀H₁₆	RI, MS
18	6-Camphenone	1099	1093	0.01	C ₁₀ H ₁₄ O	RI, MS
19	β-Linalool	1104	1100	3.04	C₁₀H₁₈O	RI, MS, AU
20	2,9-Dimethyl-5-decyne	1106	1103	0.2	C ₁₂ H ₂₂	RI, MS
21	1,3,8- <i>p</i> -Menthatriene	1114	1112	0.04	C ₁₀ H ₁₄	RI, MS
22	β -Fenchol	1117	1117	0.02	C ₁₀ H ₁₈ O	RI, MS
23	α -Campholenal	1129	1124	0.01	C ₁₀ H ₁₆ O	RI, MS
24	<i>trans</i> -Pinocarveol	1143	1140	0.05	C ₁₀ H ₁₆ O	RI, MS
25	Camphor	1149	1143	1.37	C ₁₀ H ₁₆ O	RI, MS
26	Camphene hydrate	1152	1149	0.13	C ₁₀ H ₁₈ O	RI, MS
27	Pinocarvone	1166	1161	0.04	C ₁₀ H ₁₄ O	RI, MS
28	Borneol	1170	1166	0.44	C ₁₀ H ₁₈ O	RI, MS
29	<i>p</i> -Cymen-8-ol	1188	1182	0.21	C ₁₀ H ₁₄ O	RI, MS
30	α -Terpineol	1194	1190	0.21	C ₁₀ H ₁₈ O	RI, MS
31	Myrtenal	1200	1192	0.13	C ₁₀ H ₁₄ O	RI, MS
32	<i>trans</i> -Piperitol	1211	1205	Tr.	C ₁₀ H ₁₈ O	RI, MS
33	Fenchyl acetate	1223	1219	0.06	C ₁₂ H ₂₀ O ₂	RI, MS
34	<i>cis</i> -Carveol	1227	1229	0.05	C ₁₀ H ₁₆ O	RI, MS
35	Neral	1245	1242	0.04	C ₁₀ H ₁₆ O	RI, MS
36	Linalyl acetate	1251	1255	0.06	C ₁₂ H ₂₀ O ₂	RI, MS
37	<i>trans</i> -2-Decenal	1260	1263	0.37	C ₁₀ H ₁₈ O	RI, MS
38	Geranial	1276	1270	0.05	C ₁₀ H ₁₆ O	RI, MS
39	<i>trans</i> -Cinnamaldehyde	1277	1271	0.07	C ₉ H ₈ O	RI, MS
40	Methyl hydrocinnamate	1281	1280	0.18	C ₁₀ H ₁₂ O ₂	RI, MS
41	Bornyl acetate	1292	1291	0.08	C ₁₂ H ₂₀ O ₂	RI, MS
42	2-Undecanone	1297	1293	0.05	C ₁₁ H ₂₂ O	RI, MS
43	(<i>Z</i>)-Methyl cinnamate	1305	1300	0.62	C ₁₀ H ₁₀ O ₂	RI, MS
44	(<i>E,E</i>)-2,4-Decadienal	1321	1318	0.05	C ₁₀ H ₁₆ O	RI, MS
45	Myrtenyl acetate	1331	1329	0.07	C ₁₂ H ₁₈ O ₂	RI, MS
46	α -Cubebene	1355	1351	0.52	C ₁₅ H ₂₄	RI, MS
47	α -Copaene	1381	1377	0.82	C ₁₅ H ₂₄	RI, MS
48	Methyl cinnamate	1400	1399	29.21	C₁₀H₁₀O₂	RI, MS
49	β -Caryophyllene	1430	1428	2.17	C ₁₅ H ₂₄	RI, MS, AU
50	γ -Elemene	1435	1436	0.02	C ₁₅ H ₂₄	RI, MS

51	<i>trans</i> - α -Bergamotene	1442	1436	0.19	C ₁₅ H ₂₄	RI, MS
52	α -Guaiene	1446	1440	0.32	C ₁₅ H ₂₄	RI, MS
53	Aristolene	1452	1450	2.07	C ₁₅ H ₂₄	RI, MS
54	β -Chamigrene	1458	1451	0.45	C ₁₅ H ₂₄	RI, MS
55	α -Humulene	1464	1457	0.72	C ₁₅ H ₂₄	RI, MS
56	Alloaromadendrene	1471	1465	0.69	C ₁₅ H ₂₄	RI, MS
57	δ -Selinene	1485	1485	1.09	C ₁₅ H ₂₄	RI, MS
58	Germacrene D	1492	1490	0.27	C ₁₅ H ₂₄	RI, MS
59	β -Eudesmene	1495	1490	0.39	C ₁₅ H ₂₄	RI, MS
60	α -Selinene	1498	1498	0.51	C ₁₅ H ₂₄	RI, MS
61	α -Bulnesene	1500	1504	0.40	C ₁₅ H ₂₄	RI, MS
62	Valencene	1506	1503	1.81	C ₁₅ H ₂₄	RI, MS
63	α -Muurolene	1510	1509	0.92	C ₁₅ H ₂₄	RI, MS
64	Selina-3,7(11)-diene	1530	1532	0.38	C ₁₅ H ₂₄	RI, MS
65	δ-Cadinene	1536	1530	7.05	C ₁₅ H ₂₄	RI, MS
66	α -Cadinene	1547	1546	0.07	C ₁₅ H ₂₄	RI, MS
67	<i>trans</i> -Nerolidol	1571	1564	2.31	C ₁₅ H ₂₆ O	RI, MS
68	Globulol	1585	1582	1.18	C ₁₅ H ₂₆ O	RI, MS
69	Spathulenol	1590	1591	1.19	C ₁₅ H ₂₄ O	RI, MS
70	Viridiflorol	1596	1591	1.18	C ₁₅ H ₂₄ O	RI, MS
71	Cubedol	1610		2.22	C ₁₅ H ₂₆ O	MS
72	γ -eudesmol	1634	1631	0.28	C ₁₅ H ₂₆ O	RI, MS
73	α -Cadinol	1655	1653	1.95	C ₁₅ H ₂₆ O	RI, MS
74	7(11)-Selinen-4- α -ol	1676	1675	0.38	C ₁₅ H ₂₆ O	RI, MS
75	Bulnesol	1683	1678	1.07	C ₁₅ H ₂₆ O	RI, MS
76	(<i>E,E</i>)-Farnesal	1749	1741	0.02	C ₁₅ H ₂₄ O	RI, MS
77	<i>n</i> -Octadecane	1797	1800	0.01	C ₁₈ H ₃₈	RI, MS
78	Isopropyl myristate	1825	1827	0.02	C ₁₇ H ₃₄ O ₂	RI, MS
79	Hexahydrofarnesyl acetone	1846	1848	0.01	C ₁₈ H ₃₆ O	RI, MS
80	<i>n</i> -Hexadecanol	1882	1880	0.02	C ₁₆ H ₃₄ O	RI, MS
81	<i>n</i> -Nonadecane	1899	1900	0.02	C ₁₉ H ₄₀	RI, MS
82	(<i>E,E</i>)-Farnesyl acetone	1923	1922	0.08	C ₁₈ H ₃₀ O	RI, MS
83	Palmitic acid	1965	1961	0.01	C ₁₆ H ₃₂ O ₂	RI, MS, AU
84	(<i>Z</i>)-9-Octadecenal	1996	1995	0.02	C ₁₈ H ₃₄ O	RI, MS
85	Octadecanal	2022	2021	0.20	C ₁₈ H ₃₆ O	RI, MS
86	Phytol	2122	2116	1.18	C ₂₀ H ₄₀ O	RI, MS
87	<i>n</i> -Tricosane	2301	2300	0.05	C ₂₃ H ₄₈	RI, MS
88	<i>n</i> -Tetracosane	2395	2400	0.04	C ₂₄ H ₅₀	RI, MS
89	<i>n</i> -Hexacosane	2601	2600	0.02	C ₂₆ H ₅₄	RI, MS
90	<i>n</i> -Heptacosane	2699	2700	0.07	C ₂₇ H ₅₆	RI, MS
Total				96.63%		

^aCompounds are listed according to elution order, RI ^b Kovats retention index calculated on Rtx-5MS fused bonded column, ^c Average of three analyses. MS, mass spectral data; RI, published retention indices; AU, co-chromatography with authentics, Tr., traces < 0.01. The major components are bold highlighted.

Antimicrobial activity

Inhibition zone and MIC determinations

The mean inhibition zone diameters (of three measurements) of the nanoemulsion and the clindamycin disc (2 μ g/disc) are shown in Table 3. No growth inhibition was observed in the control well (Tween-80 in water at the same used concentration). MIC value of the nanoemulsion was 62.5 μ L/mL that is equivalent to 0.61 μ L/mL of pure essential oil.

Morphological analysis by TEM

The impact of ginger leaves nanoemulsion on the destruction of the biofilm integrity of *S. mutans* was illustrated by TEM, as shown in Figure 3. The control of bacterial suspension showed cells aggregation and clumping with a chain-forming pattern. While, the bacterial suspension treated with the nanoemulsion (at its MIC level) showed significant cells scattering and dispersion without any apparent chain formation, suggesting

reduced *S. mutans* glucan synthesis, which is required for bacterial adherence (Hasan *et al.*, 2015), also the cells scattering has resulted in reduced cells interaction and impaired formation of the bacterial biofilm.

Table 2: Stability study parameters of the prepared nanoemulsion.

Days	Particle size (nm) (mean \pm SD)	Polydispersity index (mean \pm SD)	Zeta potential (mV) (mean \pm SD)
Day 0	151.4 \pm 17.38	0.268 \pm 0.003	-13.75 \pm 3.18
Day 14	153.8 \pm 11.99	0.263 \pm 0.017	-14.6 \pm 0.62
Day 30	157.6 \pm 16.26	0.258 \pm 0.030	-10.47 \pm 1.18

All measurements are done in triplicates.

Table 3: Antibacterial activity of ginger leaves oil nanoemulsion against *S. mutans*.

Tested sample	Inhibition zone diameter (mm) (mean \pm SD)*	MIC (μ L/mL)
Nanoemulsion (100 μ L)	25 \pm 1.0	62.5
Clindamycin (2 μ g/disc)	30 \pm 0.5	NT
Blank control (100 μ L)	0 \pm 0.0	NT

*Values for three determinations; NT: not tested.

Docking study

The molecular docking was done to evaluate the possible binding mode of methyl cinnamate (the major volatile component, 29.21%) to the active site of the C-terminal region of *S. mutans* surface protein antigen (Ag I/II). Inspection of the active site of the bacterial protein surface antigen revealed many amino acids, such as Glu 1215, Glu 1216, Lys1299 and Thr 1244, which stabilize

the complex of methyl cinnamate with the protein. The C-Docker binding energy of the selected docking pose was -8.239 kcal/mol. The 2D- and 3D-binding modes of methyl cinnamate are shown in Figure 4, where methyl cinnamate showed a good binding affinity to the bacterial surface protein antigen through a *Pi-Pi* interaction between the benzene ring of the ligand and the Lys 1299 residue of the protein, besides four hydrophobic interactions of the ligand with the protein active site. This indicates a high inhibitory activity of *S. mutans* surface protein antigen.

The docking results of methyl cinnamate (ginger leaves oil major component) were comparable to those reported for eugenol (the major clove oil component) on *S. mutans* surface antigen (Ag I/II) (Adil, 2013), where the amino acid residues Glu 1215 and Glu 1216 were common in stabilizing the complex formed for either compound. Moreover, eugenol bondings with the protein active site were through hydrophobic interactions as for methyl cinnamate, in addition to H-bonding.

Eugenol had been used extensively as an antiseptic, reported for its antibacterial activity against *S. mutans* (Freires *et al.*, 2015), used in dentistry as a base for fillings, and as a cement component for sealing cavities (Souza-Costa *et al.*, 2007). On the other side, methyl cinnamate has been used in many foods, pharmaceutical industries and cosmetic products (Bathia *et al.*, 2007). According to the results declared by the Joint FAO/WHO Expert Committee on Food Additives (JECFA) and the European Food Safety Authority (EFSA, 2009), methyl cinnamate intake is considered safe at the levels of use as a flavoring agent. Thus, further studies should be carried out to study the possible use of the ginger oil rich in methyl cinnamate or the pure compound in dentistry clinical applications.

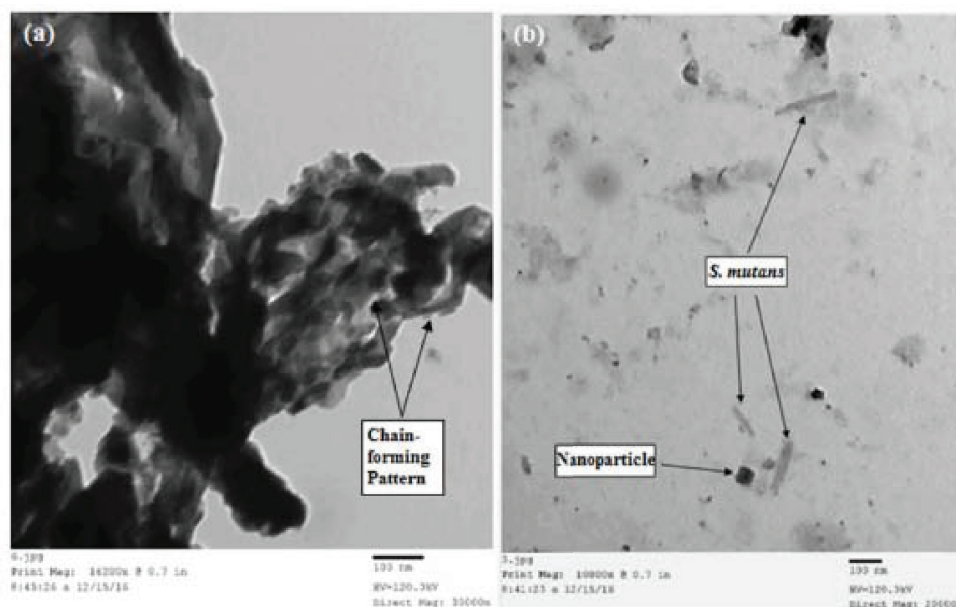


Fig. 3: Transmission electron microscope imaging of (a) *Streptococcus mutans* suspension alone showing biofilm and chain-forming aggregates, and (b) nanoemulsion (at MIC level) and *S. mutans* showing impairment of bacterial biofilm integrity. Samples magnifications were 30000 and 20000 times, respectively.

CONCLUSION

Ginger (*Zingiber officinale* Roscoe) leaves volatile oil is rich in valuable phytoconstituents; the oil nanoemulsion

formulation was stable, effective on *Streptococcus mutans*, and can be further studied for use as a gargle against dental caries and plaque formation.

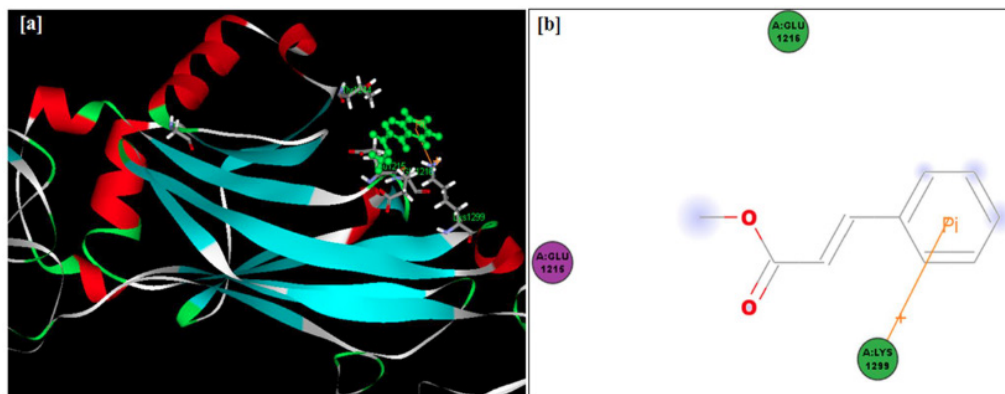


Fig. 4: Binding of methyl cinnamate to the active C-terminal region of *S. mutans* surface protein antigen in [a] 3D-diagram and [b] 2D-diagram.

CONFLICT OF INTERESTS

The author declares no conflict of interest.

ACKNOWLEDGMENTS

Thanks to Dr. Samar Samir, Lecturer of Microbiology, Faculty of Science, Ain Shams University, Cairo, Egypt, for her kind help in the antibacterial activity assessment.

REFERENCES

- Abdel-Azeem AS, Hegazy AM, Ibrahim KS, Farrag AR, El-Sayed EM. Hepatoprotective, antioxidant, and ameliorative effects of ginger (*Zingiber officinale* Roscoe) and vitamin E in acetaminophen treated rats. *J Diet Suppl*, 2013; 10:195-209.
- Adil M (Ph. D thesis). 2013. Characterization of anti-biofilm and anti-adherent compounds against *Streptococcus mutans* from medicinal plants, Interdisciplinary Biotechnology Unit, Aligarh Muslim University, India.
- Amaral DMF, Bhargava K. Essential oil nanoemulsions and food applications. *Adv Food Technol Nutr Sci Open J*, 2015; 1:84-87.
- Ayoub N, Singab AN, Mostafa N, Schultze W. Volatile constituents of leaves of *Ficus carica* Linn. grown in Egypt. *J Essent Oil Bear Pl*, 2010; 13:316-321.
- Bhatia SP, Wellington GA, Cocchiara J, Lalko J, Letizia CS, Api AM. Fragrance material review on methyl cinnamate. *Food Chem Toxicol*, 2007; 45 Suppl 1:S113-119.
- Clinical and Laboratory Standards Institute (CLSI). 2015. Methods for dilution antimicrobial susceptibility tests for bacteria that grow aerobically, approved standard-Tenth edition, M07-A10. Wayne, PA.
- Clinical and Laboratory Standards Institute (CLSI). 2013. Performance standards for antimicrobial susceptibility testing, Disc diffusion supplemental tables, M100-S23 (M02-A11). Wayne, PA.
- EFSA; Scientific Opinion on Flavouring Group Evaluation 68 (FGE.68): Consideration of cinnamyl alcohol and related flavouring agents evaluated by JECFA (55th meeting) structurally related to aryl-substituted saturated and unsaturated primary alcohol/aldehyde/acid/ester derivatives evaluated by EFSA in FGE.15Rev1 (2008). *EFSA Journal*, 2009; 7:1032.
- Flores FC, Ribeiro RF, Ourique AF, Rolim CMB, Silva CB, Pohlmann AR, Beck RCR, Guterres SS. Nanostructured systems containing an essential oil: protection against volatilization. *Quim Nova*, 2011; 34:968-972.
- Freires IA, Denny C, Benso B, de Alencar SM, Rosalen PL. Antibacterial activity of essential oils and their isolated constituents against cariogenic bacteria: A systematic review. *Molecules*, 2015; 20:7329-7358.
- Hasan S, Danishuddin M, Khan AU. Inhibitory effect of *Zingiber officinale* towards *Streptococcus mutans* virulence and caries development: *in vitro* and *in vivo* studies. *BMC Microbiol*, 2015; 15:1.

Hasan S, Singh K, Danisuddin M, Verma PK, Khan AU. Inhibition of major virulence pathways of *Streptococcus mutans* by quercitrin and deoxyojirimycin: A synergistic approach of infection control. *PLoS One*, 2014; 9:e91736.

Ishak RAH, Mostafa NM, Kamel AO. Stealth lipid polymer hybrid nanoparticles loaded with rutin for effective brain delivery – comparative study with the gold standard (Tween 80): optimization, characterization and biodistribution, *Drug Deliv*, 2017; 24:1874-1890.

Jeena K, Liju VB, Kuttan R. Antioxidant, anti-inflammatory and antinociceptive activities of essential oil from ginger. *Indian J Physiol Pharmacol*, 2013; 57:51-62.

Krzyściak W, Jurczak A, Kościelniak D, Bystrowska B, Skalniak A. The virulence of *Streptococcus mutans* and the ability to form biofilms. *Eur J Clin Microbiol Infect Dis*, 2014; 33:499-515.

Loesche WJ. Role of *Streptococcus mutans* in human dental decay. *Microbiol Rev*, 1986; 50:353-380.

Manconi M, Sinico C, Caddeo C, Vila AO, Valenti D, Fadda AM. Penetration enhancer containing vesicles as carriers for dermal delivery of tretinoin. *Int J Pharm*, 2011; 412:37-46.

Mostafa NM. β -Amyrin rich *Bombax ceiba* leaf extract with potential neuroprotective activity against scopolamine-induced memory impairment in rats. *Rec Nat Prod*, 2018; 12:480-492.

Mostafa NM, Eldahshan OA, Singab AB. Chemical composition and antimicrobial activity of flower essential oil of *Jacaranda acutifolia* Humb. and Bonpl. against food-borne pathogens. *European J Med Plants*, 2015; 6:62-69.

Mostafa NM, Singab AN. After HCV eradication with Sovaldi®, can herbs regenerate damaged liver, minimize side effects and reduce the bill? *Med Aromat Plants*, 2016; 5:257.

Nantarat T, Chansakaow S, Leelapornpisid P. Optimization, characterization and stability of essential oils blend loaded nanoemulsions by PIC technique for anti-tyrosinase activity. *Int J Pharm Pharm Sci*, 2015; 7:1491.

Nielsen CK, Kjems J, Mygind T, Snabe T, Meyer RL. Effects of Tween 80 on growth and biofilm formation in laboratory media. *Front Microbiol*, 2016; 7:1878.

Salama HH, El-Sayed MM, El-Salam MH. Preparation of β -carotene enriched nanoemulsion by spontaneous emulsification using oleic acid as nano carrier. *Res J Pharm Biol Chem Sci*, 2016; 7:585-593.

Sari M, Biondi DM, Kaabeche M, Mandalari G, D'Arrigo M, Bisignano G. Chemical composition, antimicrobial and antioxidant activities of the essential oil of several populations of Algerian *Origanum glandulosum* Desf. *Flavour Fragr J*, 2006; 21:890-898.

Singab AB, Mostafa NM, Eldahshan OA, Ashour ML, Wink M. Profile of volatile components of hydrodistilled and extracted leaves of *Jacaranda acutifolia* and their antimicrobial activity against foodborne pathogens. *Nat Prod Commun*, 2014; 9:1007-1010.

Sivasothy Y, Chong WK, Abdul Hamid, Eldeen IM, Sulaiman SF, Awang K. Essential oils of *Zingiber officinale* var. rubrum Theilade and their antibacterial activities. Food Chem, 2011; 124:514-517.

Souza-Costa CA, Teixeira HM, Nascimento ABL, Hebling J. Biocompatibility of resin-based dental materials applied as liners in deep cavities prepared in human teeth. J Biomed Mater Res B, 2007; 81:175-184.

Yang Z, Yang W, Peng Q, He Q, Feng Y, Luo S, Yu Z. Volatile phytochemical composition of rhizome of ginger after extraction by headspace solid-phase microextraction, petroleum ether extraction and

steam distillation extraction. Bangladesh J Pharmacol, 2009; 4:136-143.

How to cite this article:

Mostafa NM. Antibacterial Activity of Ginger (*Zingiber officinale*) Leaves Essential Oil Nanoemulsion against the Cariogenic *Streptococcus mutans*. J App Pharm Sci, 2018; 8(09): 034-041.